# 79

# Spectral Element Simulations of Laminar Diffusion Flames

Ullrich Becker-Lemgau and Catherine Mavriplis

## 1 Introduction

Soot generation is, in the sense of efficiency, a major problem during combustion of hydrocarbons. In order to optimize the design of combustion chambers and avoid soot generation, it is essential to understand the mechanisms of soot growth. In particular, the interactions between chemistry and fluid flow are critically important: experiments have shown that soot production is strongly dependent on the flow situation. The amount of soot generated by laminar diffusion flames is greatly enhanced if the flame becomes unstable [SHJP93, SHS94].

In order to further investigate vortex-chemistry interaction, we develop here a numerical simulation since computations allow us to investigate a wide range of destabilizing effects on laminar flames, both individually and together. In this paper we present spectral element simulations of laminar axisymmetric non-premixed methane-air diffusion flames. The spectral element method [Pat84] is a high-order domain decomposition method which is used in the solution of time-dependent nonlinear partial differential equations. The method has been used in the solution of the Navier-Stokes equations for direct simulation of fluid flow, e.g. [Kar90, FR94]. Here, we extend the Navier-Stokes solver to include chemistry and energy conservation equations. This paper is the first attempt at establishing our simulation capability for laminar diffusion flames. Results are compared with theoretical and experimental flames.

*Ninth International Conference on Domain Decomposition Methods*
Editor Petter E. Bjørstad, Magne S. Espedal and David E. Keyes

## 2 Governing Equations

The flow underlying an unsteady laminar diffusion flame is a one phase flow with variable density and viscosity due to the temperature change in the flow. It is described by the Navier-Stokes equations:

$$\frac{\partial \rho}{\partial t} + \boldsymbol{\nabla} \cdot \rho \boldsymbol{v} = 0$$

$$\rho \frac{\partial \boldsymbol{v}}{\partial t} + \rho(\boldsymbol{v} \cdot \boldsymbol{\nabla})\boldsymbol{v} = (\boldsymbol{\nabla} \cdot \mu \boldsymbol{\nabla})\boldsymbol{v} - \boldsymbol{\nabla} p + \boldsymbol{S}_v$$

with velocity $\boldsymbol{v}$, pressure $p$, density $\rho$, viscosity $\mu$ and a source term $\boldsymbol{S}_v$ which contains the buoyancy force.

The mixing process of fuel and oxygen is described by the mixture fraction $\xi$ which is a conserved scalar for the flow [Spa79]:

$$\rho \frac{\partial \xi}{\partial t} + \rho(\boldsymbol{v} \cdot \boldsymbol{\nabla})\xi = (\boldsymbol{\nabla} \cdot \rho D \boldsymbol{\nabla})\xi$$

with $D$ as the diffusivity. We assume a complete and fast one step reaction from fuel mixed with oxygen to a product mixture without intermediate products and no back reaction.

The energy equation may be expressed in terms of temperature assuming constant heat capacity:

$$c_p \rho \frac{\partial T}{\partial t} + c_p \rho(\boldsymbol{v} \cdot \boldsymbol{\nabla})T = (\boldsymbol{\nabla} \cdot k \boldsymbol{\nabla})T + Q(\xi)$$

with $k$ as conductivity and $Q$ as heat release depending on mixture fraction and flame height. We use experimental data of a methane-air flame for the heat release description [SMP96].

The system of equations is closed by the equation of state:

$$\rho = \frac{M \cdot p}{R \cdot T}$$

where $M$ is the molar weight of the gas mixture and $R$ the gas constant.

## 3 Spectral Element Model

In order to reduce the complexity of the system of equations we assume at first a flow with constant density and constant properties. So we solve the incompressible Navier-Stokes equations and will let density vary for the buoyancy term only.

The Navier-Stokes equations pose the largest problem since they have nonlinear terms and we need to incorporate the continuity equation. Therefore a multi-fractional time-stepping scheme is introduced which breaks up the equation, treating the nonlinear convection terms separately from the elliptic diffusion terms [OK80]:

$$\frac{\hat{u} - \boldsymbol{u}^n}{\Delta t} = \boldsymbol{u} \cdot \nabla \boldsymbol{u}$$

$$\nabla^2 p = \frac{\rho}{\Delta t} \nabla \cdot \hat{u}$$

$$\frac{\hat{\hat{u}} - \hat{u}}{\Delta t} = -\frac{1}{\rho} \nabla p$$

$$\frac{\boldsymbol{u}^{n+1} - \hat{\hat{u}}}{\Delta t} = \nu \nabla^2 \boldsymbol{u}$$

where $\hat{u}$ and $\hat{\hat{u}}$ are intermediate time step values of the velocities.

First, the nonlinear terms are treated explicitly by a 3rd-order Adams-Bashforth method. Then, the continuity and pressure steps are combined and a Poisson equation for pressure is solved implicitly. Finally, the elliptic velocity diffusion terms are solved implicitly as a Helmholtz problem.

The mixture fraction and temperature equations do not pose such difficulties: the advection terms are easily handled explicitly and we solve also Helmholtz problems for $\xi$ and $T$. So we have five (in 2D) Helmholtz equations to solve implicitly for velocities (two), pressure, mixture fraction and temperature.

We illustrate the spectral element discretisation for simplicity with the Poisson equation:

$$\nabla^2 u = f.$$

Starting from the Poisson equation we use the weak form (or variational form), i.e. we have to find a solution $u$ which satisfies

$$(\nabla u, \nabla v) = (f, v) \quad \forall v.$$

The physical domain is then subdivided into large elements $k$ upon each of which unknowns $u$ and knowns like $f$ are described as tensor products of high-order orthogonal functions:

$$u_h^k = u_{ij}^k h_i(r) h_j(s),$$

$$f_h^k = f_{ij}^k h_i(r) h_j(s),$$

where $h_i$'s are high-order Lagrangian interpolants based on Legendre polynomials (typically order 7).

So the discrete problem is to find the discrete solution $u_h^k$ on each element satisfying

$$(\nabla u_h^k, \nabla v_h^k)_{GL} = (f_h^k, v_h^k)_{GL} \; \forall v_h^k,$$

where the inner products are done by Gauss-Lobatto quadrature. Finally the contributions from all connecting elements are summed up. This leads to a global matrix equation $Au = Bf$ which is solved by preconditioned conjugate gradient iteration.

## 4 Validation

To validate our model we first try to compare results to a theoretical solution of a given flame. Several simplifying assumptions are necessary to solve the equations theoretically which will lead to the classical Burke-Schumann flame [BS28].

**Figure 1** Burke-Schumann flame: design and flame shapes for over- and underventilated flow situations

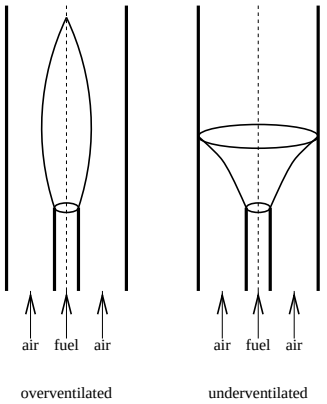


**Figure 2** Burke-Schumann flame: comparison of theoretically (dotted lines) and numerically (solid lines) obtained flame shapes for underventilated (leftmost) and overventilated flow situations

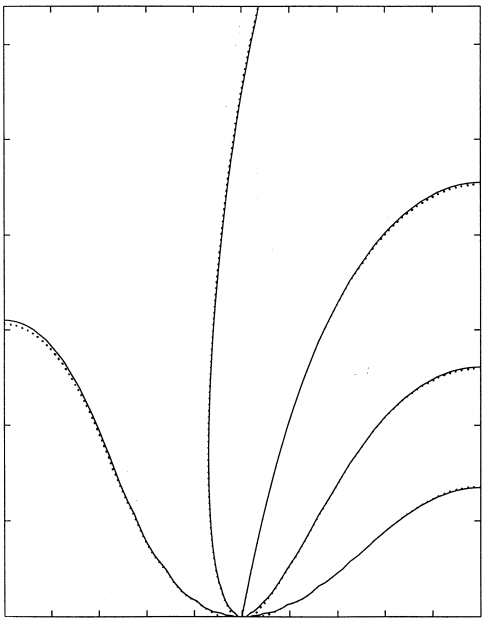

Fuel flows through a pipe into a concentric pipe with coflowing air (see Fig. 1). Velocities and properties are assumed to be uniform throughout the domain. The mixing process starts right at the outlet of the fuel pipe and thus the fast one step reaction takes place in a very thin layer.

Two classes of flames are distinguished depending on the fuel type: an overventilated flame where oxygen is in excess and all fuel is consumed by the reaction and an underventilated flame where fuel is in excess and all oxygen is consumed by the reaction. Fig. 1 shows typical flame shapes for both situations.

A comparison of theoretically and numerically obtained flame shapes can be seen in Fig. 2. Due to symmetry only the left half of the pipe is calculated and shown. Fuel is flowing into the domain from the right half of the lower edge. The co-flowing air is entering through the left half. Four overventilated and one underventilated (the leftmost) flame shapes are shown and are found to be in very good agreement with theoretical results.

## 5 Results

The geometry underlying our calculations is adapted from experiments concerning soot generation in flickering flames [SHJP93, SHS94, SMP96]. It is similar to the geometry of the Burke-Schumann flame (Fig. 1). An axisymmetric tube of diameter 1.1 cm provides the methane fuel flow into a concentric tube of diameter 10.2 cm providing co-flowing air. At the inlet of the fuel pipe a parabolic velocity profile is assumed with a maximum velocity of 12 cm/s. The co-flowing air stream has a uniform velocity of 10.4 cm/s. Because of the axisymmetric design we only have to calculate a two dimensional slice of the pipe.

In the following we will present example calculations representing our approach building a laminar diffusion flame modeling capability.

### *Calculation with Constant Properties*

The heavy coupling of the equations, especially the heat release term in the energy equation and the buoyancy term in the vertical momentum equation, makes it difficult to arrive at a suitable base solution from which we may start pulsing the flame. Therefore we start our calculations with a steady, incompressible flame and constant properties: $\rho = 0.1\,\mathrm{kg/m^3}$, $\mu = 2 \cdot 10^{-5}\,\mathrm{kg/m\,s}$, $c_p = 1000\,\mathrm{J/kg\,K}$, $k = 0.01\,\mathrm{J/m\,s\,K}$, $D = 1 \cdot 10^{-4}\,\mathrm{m^2/s}$. These values are chosen to fulfill the requirement of equal Prandtl and Schmidt numbers for diffusion flames. The Reynolds number based on the average velocity of 10 cm/s and the diameter of the air stream is $\mathrm{Re} = 51$. Because of the constant density no buoyancy is taken into account and the calculated temperatures have no influence on the fluid flow. For the heat release function in the temperature equation a simplified linear model is chosen.

The calculation domain is split into 67 spectral elements (see Fig. 3). The geometrical discontinuities between the fuel and air tubes require a domain decomposition with fine resolution around this interface region. So two narrow slices of elements are placed along the air inlet and between the air and fuel streams.

Fig. 3 (a) shows calculated axial velocity profiles at several cross-sections. The two

**Figure 3** Results for calculation with constant properties: (a) profiles of axial velocity, (b) contour lines for mixture fraction $\xi$, (c) contour lines for temperature distribution

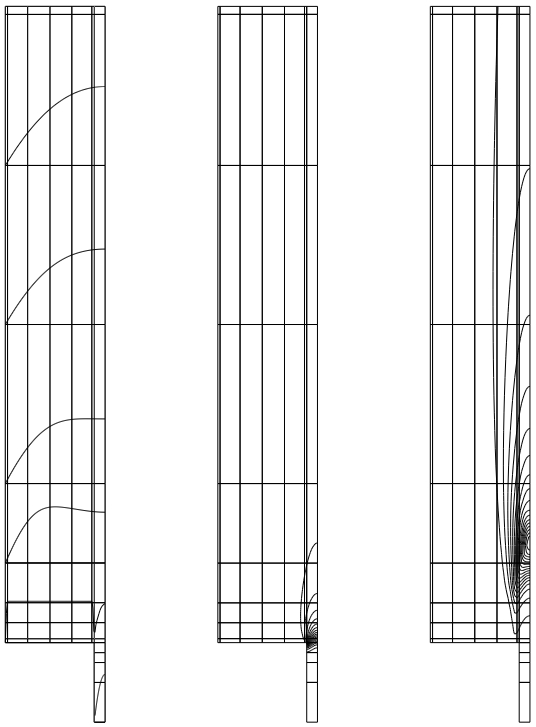


different profiles of the incoming fuel and air streams level out very quickly and a regular pipe flow profile is obtained towards the outlet.

The contour lines for the mixture fraction distribution (Fig. 3 (b)) imply a fast diffusion of oxygen into the fuel stream. The outmost contour line represents the value of $\xi$ for which methane and air are in a stoichiometric proportion. Because we assume a fast and one step reaction, this line indicates the flame shape where both fuel and oxygen are completly consumed by the reaction. The flame height is 5 cm, that is somewhat smaller than the observed flame height of 8 cm from the experiments [SMP96] due to our simplifying assumptions.

The temperature distribution (Fig. 3 (c)) is typical for a laminar diffusion flame. High temperatures are reached along the flame shape and especially at the flame tip.

As a first approach to calculate an unsteady flame we took this calculation and pulsed the fuel flow with a frequency of 10 Hz. But the results did not show any recirculation or separation as had been observed during the experiments. The

**Figure 4** Results for calculation with variable properties: (a) profiles of axial velocity, (b) contour lines for mixture fraction $\xi$, (c) contour lines for temperature distribution

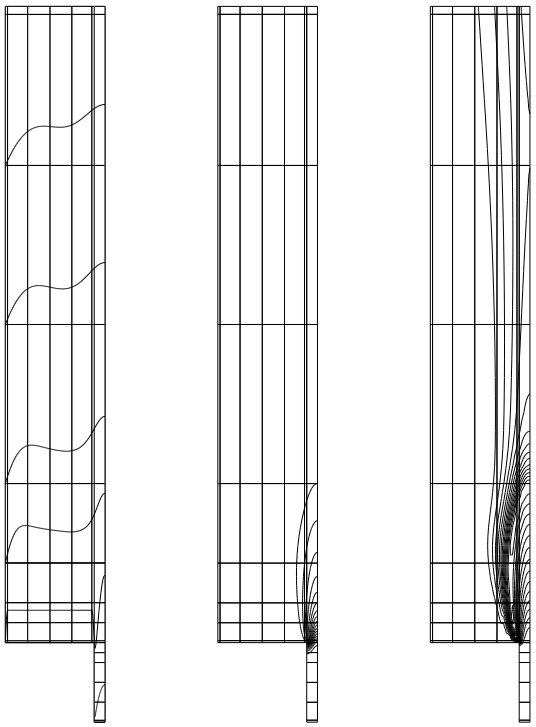

(a) (b) (c)

calculated flame height was increased to 7 cm.

*Calculation with Variable Properties and Buoyancy*

In this case we still assume a steady and incompressible flow with $\rho = 0.25\,\mathrm{kg/m^3}$ and $c_p = 1000\,\mathrm{J/kgK}$ but introduce temperature dependent properties, the models for which can be found in [SG91]:

$$\mu = 1.85 \cdot 10^{-5} \left(\frac{T}{T_0}\right)^{0.7} \frac{\mathrm{kg}}{\mathrm{m\,s}}, \qquad k = \frac{\mu c_p}{\mathrm{Pr}} \frac{\mathrm{J}}{\mathrm{m\,s\,K}}, \qquad D = \frac{\mu}{\rho\ \mathrm{Sc}} \frac{\mathrm{m}^2}{\mathrm{s}}$$

where the Prandtl number Pr and Schmidt number Sc are both equal 0.75 and $T_0$ denotes the room temperature. This gives a Reynolds number of 143 for $T = T_0$ based on velocity and diameter of the air stream. In this calculation we do not solve a temperature equation but, instead, use a temperature function $T(\xi)$ derived from

experiments [SMP96] to ensure realistic temperature values.

Variable density is introduced only for the buoyancy term. The temperature in the equation of state (see section 2) is kept constant. So the density in the buoyancy term varies only with mixture fraction in the fluid flow and pressure.

As expected, we get a speed up due to buoyancy which can be recognized by axial velocity profiles (Fig. 4 (a)). The maximum speed in the flame region is 25 cm/s. The flame height, indicated by the outmost contour line of Fig. 4 (b), is 8 cm and exactly the same as the observed flame height in the experiments.

The temperature distribution (Fig. 4 (c)) looks very similar to the one from the first calculation. But the region of the highest temperature is now spread around the flame shape and not only at the flame tip. This is caused by the temperature mixture fraction relation we used in this calculation.

## 6 Conclusion

We have shown that the spectral element method is applicable for investigations of laminar diffusion flames. Thus we have widened the range of applications for this method.

Our model was validated by very good agreement between theoretical and numerical results for the Burke-Schumann flame. For the steady flame the model is already suitable to predict flame height very well if buoyancy and variable properties are taken into account. However, calculations for the unsteady flame have not led to comparable results so far.

Further improvements are necessary for realistic predictions of the unsteady case. We have to introduce buoyancy and temperature dependent properties as for the steady flame. Also reexamination of the heat release treatment and other assumptions of the model are needed for realistic temperature distributions.

These extensions to our model will hopefully improve our results for the unsteady flickering diffusion flame in the near future.

## Acknowledgement

This work was partially supported by the George Washington University Research Enhancement Fund. Partial travel support was provided by the US National Science Foundation under Grant ECS-9209347. Support from both sources is gratefully acknowledged.

The authors would like to thank Prof. R. Goulard, Prof. J.H. Miller and Dr. M. Pivovarov from The George Washington University for fruitful discussions.

## REFERENCES

[BS28] Burke S. and Schumann T. (1928) Diffusion flames. *Indust. Eng. Chem.* 20: 998–1004.

[FR94] Fischer P. and Rønquist E. (1994) Spectral element methods for large scale

parallel navier-stokes calculations. *Computer Methods in Applied Mechanics and Engineering* 116: 69–76.

[Kar90] Karniadakis G. (1989/90) Spectral element simulations of laminar and turbulent flows in complex geometries. *Applied Numerical Mathematics* 6: 85–105.

[OK80] Orszag S. and Kells L. (1980) Transition to turbulence in plane poiseuille and plane couette flow. *Journal of Fluid Mechanics* 96: 159–205.

[Pat84] Patera A. (1984) A spectral element method for fluid dynamics: Laminar flow in a channel expansion. *Journal of Computational Physics* 54(3): 468–488.

[SG91] Smooke M. and Giovangigli V. (1991) Formulation of the premixed and nonpremixed test problems. In Smooke M. (ed) *Reduced Kintetic Mechanisms and Asymptotic Approximations for Methane-Air Flame*, volume 384 of *Lecture Notes in Physics*, pages 1–28. Springer-Verlag, Berlin.

[SHJP93] Smyth K., Harrington J., Johnsson E., and Pitts W. (1993) Greatly enhanced soot scattering in flickering $CH_4$/air diffusion flames. *Combustion and Flame* 95: 229–239.

[SHS94] Shaddix C., Harrington J., and Smyth K. (1994) Quantitative measurements of enhanced soot production in a flickering methane/air diffusion flame. *Combustion and Flame* 99: 723–732.

[SMP96] Smooke M., Miller J., and Pivovarov M. (1996) Private communications.

[Spa79] Spalding D. (1979) *Combustion and Mass Transfer*. Pergamon Press, Oxford.